J Seismol (2011) 15:355–373
DOI 10.1007/s10950-011-9229-8

ORIGINAL ARTICLE

Applications of cumulative absolute velocity to urban earthquake early warning systems

Yasin M. Fahjan · Hakan Alcik · Ali Sari

Received: 1 November 2009 / Accepted: 18 January 2011 / Published online: 10 March 2011

Abstract An early warning system forewarns an urban area of the forthcoming strong shaking, normally with a few seconds to a few tens of seconds of early warning time before the arrival of the destructive S-wave part of the strong ground motion. For urban and industrial areas susceptible to earthquake damage, where the fault rupture system is complex and the fault-site distances are short, there is usually insufficient time to compute the hypocenter, focal parameters and the magnitude of an earthquake. Therefore, simpler and robust early warning algorithm is needed. The direct (engineering) early warning systems are based on algorithms of the exceedance of specified threshold time domain amplitude levels. The continuous stations' data are processed to compute specific engineering parameters robustly and compared with specified threshold levels. The parameters can be chosen as band-pass filtered peak ground accelerations and/or the bracketed cumulative absolute velocity (BCAV). In this paper, an enhancement to bracket cumulative absolute velocity for the application of online urban early warning systems results in a new parameter called window based bracketed cumulative absolute velocity (BCAV-W). The BCAV-W allows computation of cumulative absolute velocity in a specified window size and to include the vertical component of the motion. The importance of choosing optimum window size for the cumulative absolute velocity BCAV-W is discussed and the correlations between BCAV-W and the macroseismic intensity are studied for three combinations of horizontal and vertical components of the motion. Empirical relationship is developed to estimate BCAV-W as a function of magnitude, distance, fault mechanism, and site category based on 1,208 recorded ground motion data from 75 earthquakes in active plate-margins.

Keywords Early warning system · Cumulative absolute velocity (CAV) · Attenuation relationship · Window based bracketed cumulative absolute velocity

Y. M. Fahjan (✉)
Earthquake and Structural Engineering,
Gebze Institute of Technology, Gebze,
Kocaeli, Turkey
e-mail: fahjan@gyte.edu.tr
URL: http://www.gyte.edu.tr/earthquake

H. Alcik
Kandilli Observatory and Earthquake Research
Institute, Bogazici University, 34684 Cengelkoy,
Istanbul, Turkey
e-mail: alcik@boun.edu.tr

A. Sari
ATKINS, Houston, TX, USA
e-mail: Ali.Sari@atkinsglobal.com

1 Background and introduction

Technological advances in seismic instrumentation and telecommunication permit the implementation of earthquake early warning systems that hold the potential to reduce the damaging effects of large earthquakes by giving a few seconds to tens of seconds warning before the arrival of damaging ground motion. A modern approach of an earthquake early warning system for a seismic computerized alert network was proposed by Heaton (1985). Earthquake early warning in urban and industrial areas allows for clean emergency shutdown of systems susceptible to damage such as power stations, transportation, computer centers and telephone systems. Currently, such systems are either implemented or in construction or planning stage in Mexico, Romania, California, Japan, Taiwan, Turkey. Operational early warning systems in Mexico City (Espinosa-Aranda et al. 1995; Espinoza-Aranda and Rodriquez-Cayeros 2003), Bucharest (Wenzel et al. 1999) and Taiwan (Teng et al. 1997; Wu et al. 1998; Wu and Kanamori 2005) use front detection technique to give early warning. The approach involves calculating earthquake magnitude near the source and issuing a warning to populations a greater distance away.

In the literature, many researchers studied and developed automatic processing systems to detect earthquakes and determine hypocenters, magnitudes, and focal mechanisms from P-wave and S-wave arrival times and their amplitudes (Yokota et al. 1981; Horiuchi et al. 1992; Kanamori 1993; Cansi 1995; Kanamori et al. 1997; Horiuchi et al. 2005). Nakamura (1988) developed advanced and more rapid system called UrEDAS, which uses the initial motions of the P wave recorded at a single station to determine earthquake parameters (Ashiya 2004). Allen and Kanamori (2003) have also used a P-wave detection approach to determine earthquake magnitude, but in a manner that utilizes a network of seismic stations to increase the accuracy of magnitude estimates.

Alternatively, for area with complex fault rupture and the short fault distances involved, a simple and robust early warning algorithm, based on the exceedance of specified threshold time domain amplitude levels can be used. The algorithm is generally used as an early warning for the nuclear power plants (EPRI NP-5930, 1988; EPRI TR-100082, 1991). The algorithm is based on such that the band-pass filtered peak ground accelerations (PGA) and the cumulative absolute velocity (CAV-time integral of the absolute acceleration) is compared with specified threshold levels (Erdik et al. 2003).

For nuclear power plants, as suggested by (EPRI NP-5930, 1988), CAV is used to identify earthquakes that are not potentially damaging regardless of the response spectral values. The CAV is primarily sensitive to potentially damaging low-frequency motions, but less sensitive to high-frequencies, which are generally non-damaging. This explains the high correlation between CAV and seismic intensity (EPRI NP-5930, 1988). A study by Cabanas et al. (1997) expressed the potential structural damage for building type structure using CAV by relating it with the local Intensity. Based mainly on European strong motion data, Kostov (2005) proposed a correlation between CAV and the macro-seismic intensity, magnitude and distance (attenuation functions). Based on cumulative absolute velocity, Kramer and Mitchell (2006) introduced a new ground motion intensity measure, CAV5, as an efficient, sufficient, and predictable intensity measure for rock motions used as input to liquefaction hazard evaluations. EPRI (2006), utilized CAV as filtering for hazard analyses to avoid the sensitivity to the lower bound magnitude by applying a smooth transition from not potentially damaging to potentially damaging.

In this study, the CAV is adopted for the application in triggering algorithm for urban early warning systems and a new definition suitable for such systems are proposed.

2 Direct (engineering) early warning algorithms

An earthquake early warning system requires seismic stations (strong motion instruments), which can provide real-time seismic data or strong ground motion parameters (spectrum intensities, peak ground accelerations, peak ground velocities)

close to the source of earthquakes and continuous communication between the seismic stations and a central processing station. The Early Warning Systems (EWS) utilize the fact that seismic waves propagate slower than electromagnetic waves used for the warning communications. The maximum pre-warning times in areas with well-defined fault zones can be as high as 60 to 80 s (Mexico City). In other areas, where the fault zones are close or the active faults are not known, the warning time may be less than 5 s. However, even a small time window can provide opportunities to automatically trigger measures such as shutdown computers; remote electric power; shutdown high precision facilities; shutdown airport operations; shutdown manufacturing facilities; shutdown high energy facilities; shutdown gas distribution; alert hospital operating rooms; open fire station doors; start emergency generators; stop elevators in a safe position; shutoff oil pipelines; issue audio alarms; shutdown refineries; shutdown nuclear power plans; shutoff water pipelines; maintain safe-state in nuclear facilities (Harben 1991). The earthquake early warning consists of seismic stations as close as possible to the potential source zone which transmits continuous on-line data to provide near-real time warning for emerging potentially disastrous earthquakes. Every EWS consists of four components: (1) a monitoring system composed of various sensors, (2) a real-time communication link that transmits data from the sensors to a computer, (3) a processing facility that converts data to information, and (4) a system that issues and communicates the warning. For earthquake, early warning and alarm systems there is usually insufficient time to compute the hypocenter, focal parameters and the magnitude of an earthquake, as this time is needed for the more complex alarm decision-making process. The benefits of an early warning system increase with increasing pre-warning time. Considering the complexity of fault rupture and the short fault distances involved, a simple and robust early warning algorithm, based on the exceedance of specified threshold time domain amplitude levels needs to be implemented. The band-pass filtered PGA and the cumulative absolute velocity (CAV-time integral of the absolute acceleration) can be compared with specified threshold levels. To declare the first early warning alarm, a simple algorithm can be implemented. When any acceleration or CAV (on any channel) in a given station exceeds the specific

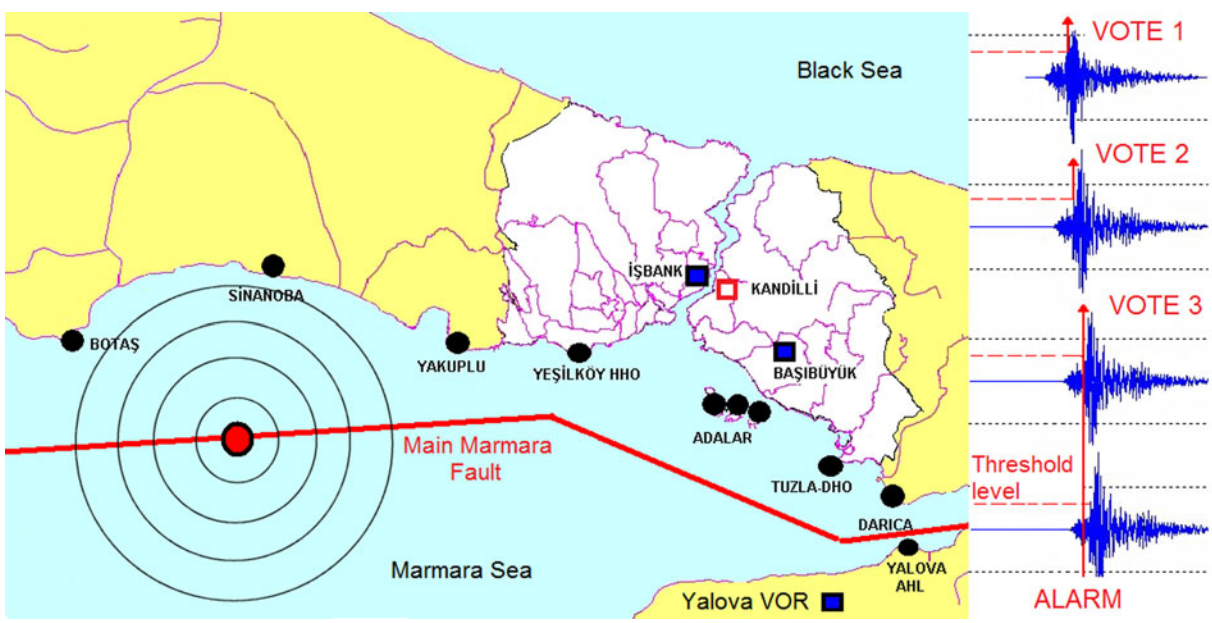

Fig. 1 Direct early warning methodology

threshold values it is considered a vote. As it is shown in Fig. 1, whenever two or three stations votes within the selectable time interval, after the first vote, the first alarm is declared (Erdik et al. 2003). For urban early warning system three level alarm algorithms can be implemented to (Alcik et al. 2006). The early warning information (consisting of three alarm levels) can be communicated to an appropriate servo shut-down systems of the recipient facilities, which will automatically decide proper action based on the alarm level.

In this approach, there is a need for the definitions of PGA and/or CAV triggering thresholds levels. For earthquake monitoring system of a nuclear power plant, the definitions of these thresholds were studied analytically and experimentally (EPRI NP-5930, 1988; EPRI TR-100082, 1991). Thresholds of PGA levels for building type structures can be defined according to specific intensity scale measurement (for example, European Macro-Seismic Scale, Modified Mercalli Scale) and the empirical values describing the peak ground acceleration for each scale. The definitions of CAV trigger level need to be studied and analyzed to be used in the early warning systems.

3 Cumulative absolute velocity for early warning algorithms

CAV is an integral quantity which depends on the entire time span from the begging of the record to a certain time t. The definitions and setting the triggering threshold levels of cumulative absolute velocity play major rule in the success of direct early warning algorithms.

3.1 Cumulative Absolute Velocity

The CAV was originally proposed by Kennedy and Reed in a study sponsored by the Electric Power Research Institute (EPRI NP-5930, 1988) as a parameter for determining the damage threshold for engineered structures and anchored industrial grade equipment subjected to earthquake ground motion. Originally, the CAV was defined as the sum of the consecutive peak-to-valley distances in the velocity time history.

$$\mathrm{CAV} = \int_0^{\mathrm{t\,max}} |\mathrm{a}\,(\mathrm{t})|\,\mathrm{dt} = \sum_0^{\mathrm{t\,max}} |\mathrm{a}\,(\mathrm{t})|\,\mathrm{dt} \tag{1}$$

Where, $a(t)$ is acceleration time history, and $t_{\max}$ = duration of record. CAV can be also interpreted as the area under the acceleration versus duration curve. EPRI (1988) investigated original database of 263 earthquake records, mainly from eastern and western U.S. and around the world. The horizontal components of each record are analyzed separately and suggested that the ground motion with CAV less than 0.30 g s would not be potentially damaging to well-engineered structures.

3.2 Bracketed Cumulative Absolute Velocity

Later on, a modified method of calculating CAV was proposed by (EPRI TR-100082, 1991) in order to remove the dependence on records of long duration containing low (non-damaging) accelerations. This result in a new parameter called bracketed cumulative absolute velocity (BCAV). The method of computing BCAV based on the summation of absolute velocity within a time domain where the max acceleration is greater than a specific value of minimum acceleration in a specific bracketed time Δt

$$\mathrm{BCAV} = \sum \int_{t_i}^{t_i+\Delta t} |a\,(t)|\;\; dt,$$

$$\Delta t = 1\,s,\ \max |a\,(t)| > 0.025\mathrm{g} \tag{2}$$

where $a(t)$ are the acceleration values in a 1 second bracket interval, and at least one value of the acceleration exceeds a predetermined threshold acceleration level (typically 0.025 g). Thus, the standard cumulative absolute velocity, CAV, becomes a discrete sum of integrals calculated in 1-s intervals. Each interval contributes to the sum only if it has at least one peak that exceeds the threshold level of acceleration. In this way, the extended lull zones of the accelerogram containing low and non-damaging amplitudes are filtered.

EPRI (1991) reanalyzed the data set used in EPRI (1988) and the adjusted threshold of damage for CAV was found to be 0.16 g s.

3.3 Window-based Bracketed Cumulative Absolute Velocity

In this study, an enhancement to the definition of BCAV is proposed for online urban early warning automatic triggering systems to account for the following operational considerations: (1) to eliminate the accumulated BCAV values due to different reasons, for examples: high noises, small earthquakes and far field events. Accumulation of BCAV values results in unwanted false alarms; therefore, an application of window-based bracketed cumulative absolute velocity (BCAV-W) is necessary to increase the system robustness. (2) To adjust the minimum acceleration level that is originally proposed for nuclear power plants. (3) To identify the short duration earthquake motions with very large peak ground accelerations (near field impulsive with duration <10 s) from long duration earthquake motions with a lower acceleration level (far field with duration >45 s).

The window-based BCAV-W can be computed as follows;

$$\text{BCAV-W} = \sum_{W=1}^{\text{winsize}} \int_{t_i}^{t_i+\Delta t} |a\,(t)|\,dt,$$

$$\Delta t = 1\,\text{s},\ \max|a\,(t)| > \text{Min Acc Level} \quad (3)$$

Where, $a(t)$ are the acceleration values in a specific bracketed time $\Delta t = 1$ s, and at least one value of the acceleration exceeds a predetermined threshold acceleration level (Min Acc Level). The discrete integration results for 1-s bracket intervals are summed for specified window size (win size). The discrete integrals summed within the window size will be continually moving over the time. To adjust the threshold level for BCAV definition, Cabanas et al. (1997) conducted several analyses using different threshold acceleration levels (25, 20, and 15 cm/s^2) and the best correlation between BCAV and damage was estimated for the second threshold. In this study, the threshold acceleration level for BCAV and BCAV-W are considered to be (0.02 g). The BCAV-W for window size 4, 8, 16, 32 are computed and compared with CAV and BCAV in Fig. 2 for horizontal component (C05085) of Cholame station #5 recorded during the 1966 Parkfield earthquake.

3.4 Triggering algorithms using different components of ground motions

The triggering algorithms can be performed using different methods dealing with the three components of the free-field ground motion (i.e., two horizontal and one vertical). In general, the maximum of the horizontal components of the motions is considered for early warning system of nuclear power plants where in most cases the seismic stations are located in the vicinity of the plant. The strategy for triggering system for urban EWS may be different in view of the fact that the seismic stations for urban EWS are generally located as close as possible to the potential fault source zone and may be far from the area under risk. To account for near- and far-field strong ground motions variation, it could be more useful to consider the effect of both horizontal and vertical components of the ground motions recorded by the seismic stations.

3.5 Maximum of horizontal components, max (H1, H2)

In most of the studies considering the triggering levels for nuclear power plants (EPRI 1988, 1991; Koliopoulos et al. 1998; Kostov 2005; Cabanas et al. 1997), the values are computed for each of the horizontal components (x, y) separately and the maximum value is considered.

$$\text{BCAV} = \text{Max}\left(\sum \int_{t_i}^{t_i+\Delta t} |a_x\,(t)|\,dt,\ \sum \int_{t_i}^{t_i+\Delta t} |a_y\,(t)|\,dt\right),$$

$$\Delta t = 1\,\text{s}, \max|a\,(t)| > 0.02\text{g} \quad (4)$$

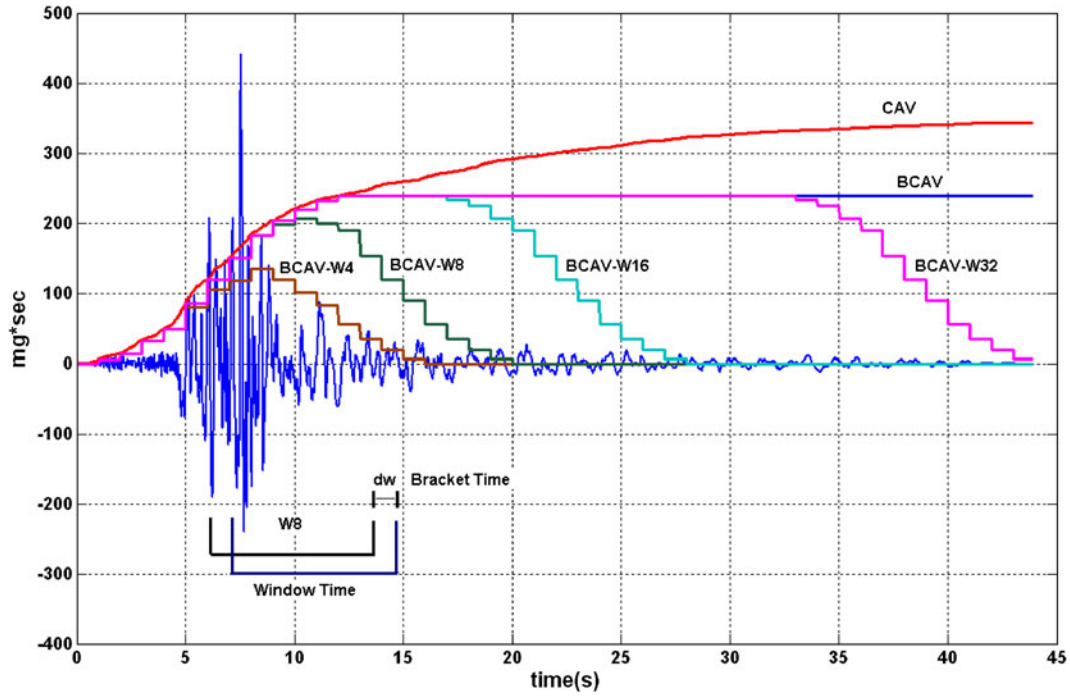

Fig. 2 Definitions of CAV, BCAV, and BCAV-W

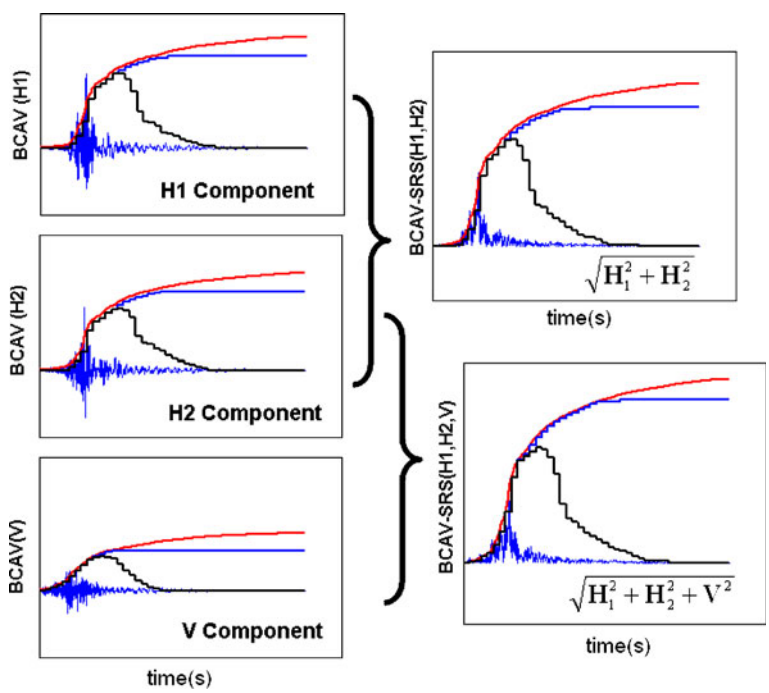

Fig. 3 Different methods to utilize different components of ground motions

Lee and Lee (2001) use a new approach for Korean nuclear power plants by computed the maximum value for both horizontal and vertical components.

3.6 Square root of sum squares of horizontal components, SRS (H1, H2)

In this approach, the square root of sum squares (SRS) of the horizontal accelerations (x, y) is calculated as shown in Fig. 3, and then BCAV is computed consequently as follows:

$$\begin{aligned} \mathrm{BCAV} &= \sum \int_{t_i}^{t_i+\Delta t} |a(t)|\, dt,\ |a(t)| \\ &= \sqrt{a_x^2(t) + a_y^2(t)}, \\ \Delta t &= 1\,\mathrm{s}, \max|a(t)| > 0.02\mathrm{g} \end{aligned} \tag{5}$$

3.7 Square root of sum squares of three components, SRS (H1, H2, V)

For urban EWS the spatial variations of motions due to near source seismic stations and far field seismic stations can be better adjusted utilizing all the three components of the motions (x, y, z). In this approach, the square root of sum squares of all the three components (two horizontal, one vertical) are calculated (Fig. 3), therefore BCAV can be computed as:

$$\begin{aligned} \mathrm{BCAV} &= \sum \int_{t_i}^{t_i+\Delta t} |a(t)|\, dt, \\ |a(t)| &= \sqrt{a_x^2(t) + a_y^2(t) + a_z^2(t)}, \\ \Delta t &= 1\,s,\ \ \max|a(t)| > 0.02\,\mathrm{g} \end{aligned} \tag{6}$$

In fact, BCAV-W includes the earthquake energy released within the specified window size; therefore, it is useful to find the ratios of BCAV-W to the total BCAV in the records for different window size. A set of time histories contains 1,320 records for crustal earthquake with different magnitude, epicentral distances, focal mechanism and soil conditions are analyzed and the relations between the window size and BCAV-W ratio for different combinations of record components are given in Fig. 4. The BCAV-W computed for different window size 4, 8, 16, and 32 s have the ratios %40, %60, %85 and 98% to the total BCAV respectively. The maximum difference between the results of different combinations of the motions components is not more than 5%. The results show that there is no significant benefit to choose a window size more than 16 s. Choosing window size less than 8 s requires new computations for the threshold alarm levels for the early

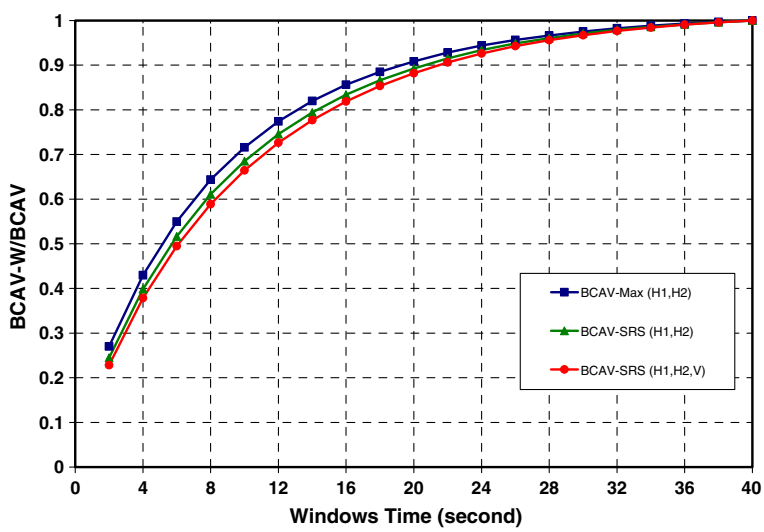

Fig. 4 Variation of BCAV-W/CAV with window size

Table 1 Earthquakes data used in correlation between BCAV-W and Modified Mercalli Intensity

Earthquake	Year/month–day/hour–second	Mw	Fault mechanism	Number of stations	Intensity range(MMI)
Kern County	1952 0721 1153	7.4	RO	1	VII
San Fernando	1971 0209 1400	6.6	R	2	VI–IX
Gazli, USSR	1976 0517	6.8	R	1	IX
Santa Barbara	1978 0813	6.0	RO	1	VII
Coyote Lake	1979 0806 1705	5.7	SS	1	VII
Imperial Valley	1979 1015 2316	6.5	SS	1	VII
Coallinga	1983 0502 2342	6.4	RO	1	VIII
Whittier Narrows	1987 1001 1442	6.0	R	33	IV–VIII
Spitak, Armenia	1988 1207	6.8	RO	1	VIII
Loma Prieta	1989 1018 0005	6.9	RO	43	VI–VIII
Erzincan, Turkey	1992 0313 1718	6.7	SS	1	IX
Northridge	1994 0117 1231	6.7	R	7	VII–VIII
Kocaeli, Turkey	1999 0817	7.4	SS	11	VI–IX

warning algorithms using BCAV-W. In the next sections, the BCAV-W relationship with intensity and BCAV-W attenuation relationships are studied in order to define an appropriate threshold alarm level for different window sizes and different combinations of ground motions.

4 Relationships between BCAV-W and intensity

In the literature, CAV was found to be well correlated with structural damage potential of earthquake ground motion (Kramer 1996; EPRI 1988) and with the local intensity. Koliopoulos et al. (1998) suggested predictive relations based on duration and energy characteristics of 53 strong shallow earthquakes in Greece with magnitude range from 4.5 up to 6.9. Utilizing the dataset of 201 horizontal accelerograms components of ground motion records, regression functions were proposed to correlate the mean values of cumulative absolute velocity, CAV, to modified Mercalli intensity, I_{mm}, as follows:

$$\ln(CAV) = 0.51\, I_{\mathrm{mm}} + 1.97\mathrm{cm/s} \quad R^2 = 0.93 \quad (7)$$

The statistical variability in the study supported the statement that CAV of 0.30 g s corresponds to the lower limit for modified Mercalli intensity (MMI) of VII shaking.

Cabanas et al. (1997) performed the regression analyses to find the relationship between BCAV and the local intensity (MSK) based on 25 three-component accelerations in different site conditions recorded by the Italian strong motion network, and have epicentral distances ranging from 6 to 128 km. For each seismic station, the records corresponding to horizontal components of greater peak acceleration were selected. The mean values of BCAV for each intensity degree, corresponding to the calculation threshold 20 cm/s^2 were determined as:

$$\ln(\mathrm{BCAV}) = 1.24 I_L - 3.54\ \mathrm{cm/s} \quad R^2 = 0.91 \quad (8)$$

Kostov (2005) analyzed the correlation between cumulative absolute velocity (BCAV) and the macro-seismic intensity, based mainly on European strong motion data (2000). The database covered most of the active seismic zones in Europe. However, the biggest part of the records is from Italian and Greek earthquakes. Utilizing 790 records with defined local intensity according

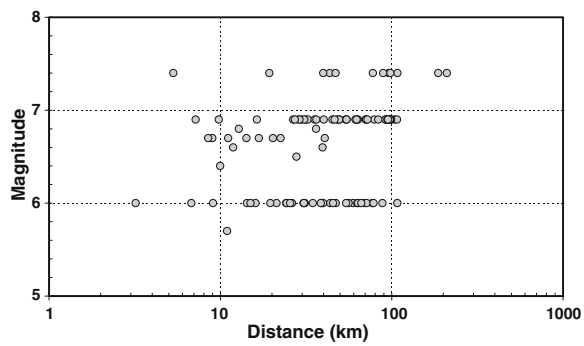

Fig. 5 Distribution of earthquakes records used in correlation between BCAV-W and MMI

Table 2 Correlation equations between BCAV-W and modified Mercalli intensity

Window size (s)	Algorithm	Equation	R^2
4	Max(H1,H2)	$\ln(\text{BCAV}-\text{W4}) = 0.454\ I_{\text{mm}} + 2.188$ cm/sec	0.465
	SRS(H1,H2)	$\ln(\text{BCAV}-\text{W4}) = 0.446\ I_{\text{mm}} + 2.593$ cm/sec	0.458
	SRS(H1,H2,V)	$\ln(\text{BCAV}-\text{W4}) = 0.455\ I_{\text{mm}} + 2.638$ cm/sec	0.463
8	Max(H1,H2)	$\ln(\text{BCAV}-\text{W8}) = 0.456\ I_{\text{mm}} + 2.584$cm/sec	0.466
	SRS(H1,H2)	$\ln(\text{BCAV}-\text{W8}) = 0.442\ I_{\text{mm}} + 3.064$cm/sec	0.463
	SRS(H1,H2,V)	$\ln(\text{BCAV}-\text{W8}) = 0.448\ I_{\text{mm}} + 3.141$cm/sec	0.460
16	Max(H1,H2)	$\ln(\text{BCAV}-\text{W16}) = 0.493\ I_{\text{mm}} + 2.568$cm/sec	0.469
	SRS(H1,H2)	$\ln(\text{BCAV}-\text{W16}) = 0.463\ I_{\text{mm}} + 3.188$cm/sec	0.454
	SRS(H1,H2,V)	$\ln(\text{BCAV}-\text{W16}) = 0.456\ I_{\text{mm}} + 3.374$cm/sec	0.441
32	Max(H1,H2)	$\ln(\text{BCAV}-\text{W32}) = 0.514\ I_{\text{mm}} + 2.495$cm/sec	0.465
	SRS(H1,H2)	$\ln(\text{BCAV}-\text{W32}) = 0.486\ I_{\text{mm}} + 3.120$cm/sec	0.449
	SRS(H1,H2,V)	$\ln(\text{BCAV}-\text{W32}) = 0.479\ I_{\text{mm}} + 3.319$cm/sec	0.435

to European Macro-seismic Scale, the BCAV with a threshold of 0.025 g was correlated as:

$$\ln(\text{BCAV}) = 0.57\ I_L - 6.3 \quad (\text{g s}) \tag{9}$$

In this study, regression analyses have been performed to determine the correlation relationships between the BCAV-W for different window size with MMI. The MMI intensity information data used in the analyses composed of different resources from the literature (Shabestari and Yamazaki 2001; EPRI 1988; Sokolov 2002; Sokolov and Chernov 2002; Ozmen 2000). The dataset includes 104 three components accelerograms (two horizontal and one vertical) from 13 earthquakes with magnitudes from 5.7 to 7.4 and MMI intensities ranging from IV to IX as given in Table 1. The fault mechanisms of the earthquakes are referred as: N for normal, SS for strike-slip, R for reverse and RO for reverse-oblique faults. The magnitudes and epicentral distances distribution

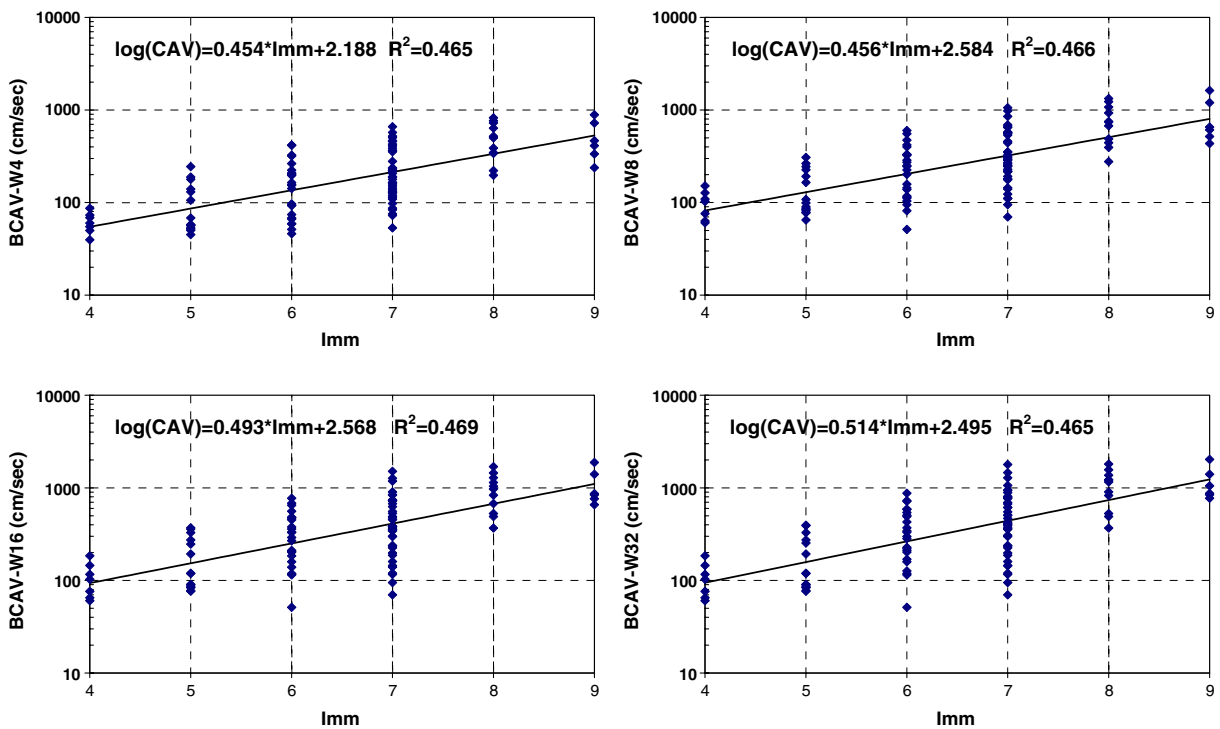

Fig. 6 Correlation between BCAV-W and MMI for Max(H1,H2) algorithm

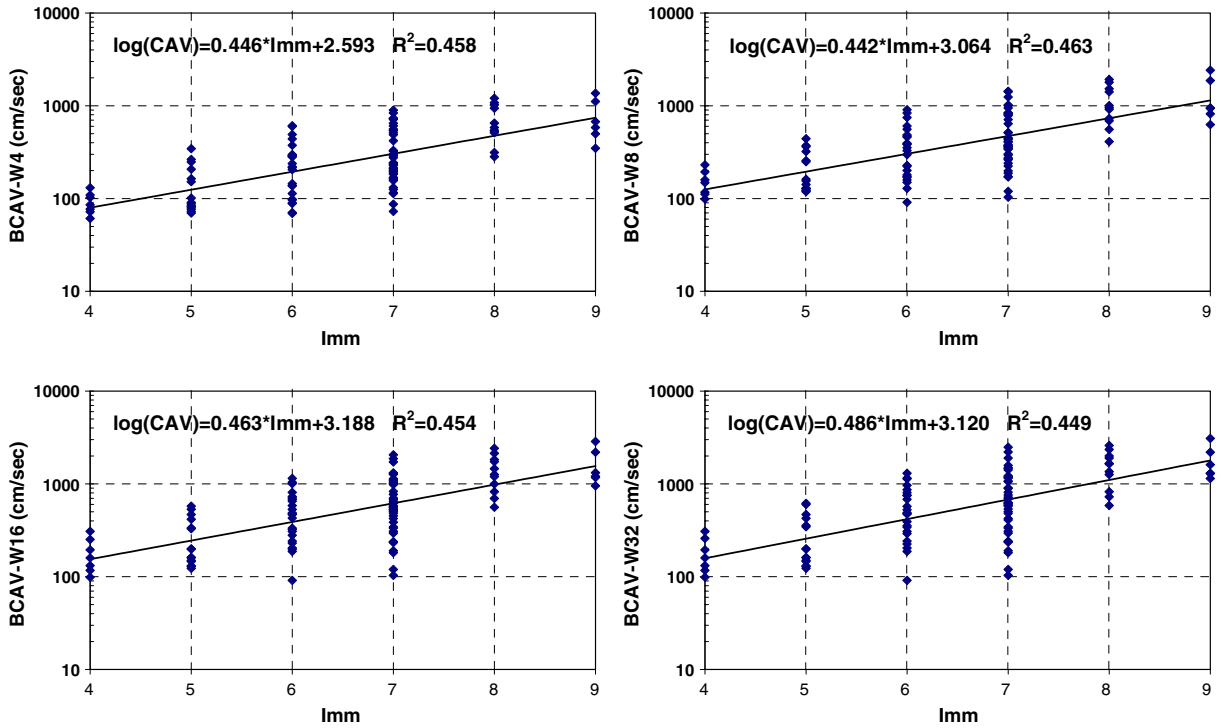

Fig. 7 Correlation between BCAV-W and MMI for SRS(H1,H2) algorithm

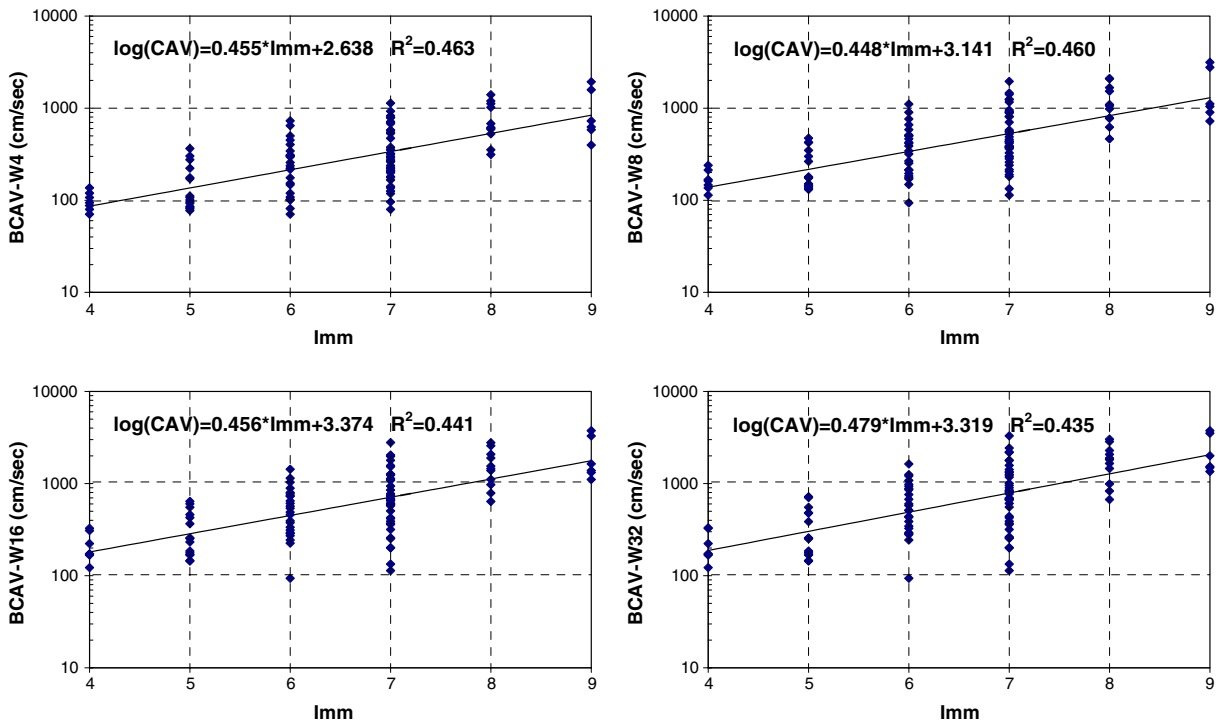

Fig. 8 Correlation between BCAV-W and MMI for SRS(H1,H2,V) algorithm

Table 3 Earthquakes data used in attenuation relationship for BCAV-W

Earthquake	Year/month–day/hour–second	Mw	Fault mechanism	Number of stations
Imperial Valley	1940 0519 0437	7.0	SS	1
Kern County	1952 0721 1153	7.4	RO	5
San Francisco	1957 0322 1944	5.3	R	1
Parkfield	1966 0628 0426	6.1	SS	5
Borrego Mountain	1968 0409 0230	6.8	SS	5
Lytle Creek	1970 0912 1430	5.4	RO	9
San Fernando	1971 0209 1400	6.6	R	42
Point Mugu	1973 0221 1445	5.8	R	1
Hollister	1974 1128 2301	5.2	SS	2
Oroville	1975 0802 2022	5.0	N	2
Oroville	1975 0808 0700	4.7	N	9
Fruili, Italy	1976 0506 2000	6.5	R	5
Gazli, USSR	1976 0517	6.8	R	1
Santa Barbara	1978 0813	6.0	RO	2
Tabas, Iran	1978 0916	7.4	R	7
Coyote Lake	1979 0806 1705	5.7	SS	10
Imperial Valley	1979 1015 2316	6.5	SS	33
Imperial Valley	1979 1015 2319	5.2	SS	16
Imperial Valley	1979 1016 0658	5.5	SS	1
Livermore	1980 0124 1900	5.8	SS	7
Livermore	1980 0127 0233	5.4	SS	8
Anza Horse Canyon	1980 0225 1047	4.9	SS	5
Mammoth Lakes	1980 0527 1901	4.9	SS	5
Mammoth Lakes	1980 0531 1516	4.9	SS	7
Victoria, Mexico	1980 0609 0328	6.4	SS	4
Mammoth Lakes	1980 0611 0441	5.0	SS	8
Irpinia, Italy	1980 1123 1834	6.9	N	12
Irpinia, Italy	1980 1123 1835	6.2	N	10
Taiwan (SMART #5)	1981 0129	5.7	R	7
Westmorland	1981 0426 1209	5.8	SS	6
Coallinga	1983 0502 2342	6.4	RO	46
Coallinga	1983 0509 0249	5.0	R	19
Coallinga	1983 0611 0309	5.3	R	3
Coallinga	1983 0709 0740	5.2	R	11
Coallinga	1983 0722 0239	5.8	R	11
Coallinga	1983 0722 0343	4.9	R	2
Coallinga	1983 0725 2231	5.2	R	2
Coallinga	1983 0909 0916	5.3	SS	2
Morgan Hill	1984 0424 2115	6.2	SS	27
Bishop (Rnd Val)	1984 1123 1912	5.8	SS	1
Nahani, Canada	1985 1223	6.8	RO	2
Hollister	1986 0126 1920	5.4	SS	3
Taiwan (SMART #40)	1986 0520	6.4	RO	8
N. Palm Springs	1986 0708 0920	6.0	RO	29
Chalfant Valley	1986 0720 1429	5.9	SS	5
Chalfant Valley	1986 0721 1442	6.2	SS	11
Chalfant Valley	1986 0721 1451	5.6	SS	3
Chalfant Valley	1986 0731 0722	5.8	SS	2
Whittier Narrows	1987 1001 1442	6.0	R	115
Whittier Narrows	1987 1004 1059	5.3	RO	11
Superstition Hills	1987 1124 0514	6.3	SS	1
Superstition Hills	1987 1124 1316	6.7	SS	3

Table 3 (continued)

Earthquake	Year/month–day/hour–second	Mw	Fault mechanism	Number of stations
Spitak, Armenia	1988 1207	6.8	RO	1
Loma Prieta	1989 1018 0005	6.9	RO	61
Erzincan, Turkey	1992 0313 1718	6.7	SS	1
Cape Mendocino	1992 0425 1806	7.1	R	6
Landers	1992 0628 1158	7.3	SS	69
Northridge	1994 0117 1231	6.7	R	147
Kobe, Japan	1995 0116 2046	6.9	SS	12
Kocaeli, Turkey	1999 0817	7.4	SS	31
Chi-Chi, Taiwan	1999 0920	7.6	R	417
Duzce, Turkey	1999 1112	7.1	SS	22

of the earthquakes records used in the correlation is plotted in Fig. 5.

Bracketed cumulative absolute velocity BCAV-W for the window sizes 4, 8, 16, and 32 s are correlated with the Modified Mercalli Intensity for different combinations of ground motion components as presented in Table 2. Plots of the correlation equations for Max(H1,H2), SRS(H1,H2) and SRS(H1,H2,V) algorithms and their fit to the data are shown in Figs. 6, 7 and 8 respectively.

5 Empirical attenuation relationship for BCAV-W

In literature, there are few studies considering the correlation between CAV, earthquake magnitude and source-station distance (attenuation functions). Kramer and Mitchell (2006) proposed a new definition of CAV called CAV5 to evaluate the liquefaction hazards. Strong-motion database included 282 records from 40 earthquakes of magnitudes between 4.7 and 7.4 was compiled from PEER strong motion database for development of a CAV5 attenuation equation. Kostov (2005), utilized the data from regional sources based mainly on the European strong-motion database to develop the attenuations for CAV and strong correlation between surface magnitude and average was found.

In this study, the attenuation relationships for bracketed cumulative absolute velocity BCAV-W with 8, 16, and 32 s window sizes are estimated for different combinations of ground motion components. The dataset used by Travasarou et al. (2003) for the attenuation relationship of Arias Intensity are utilized and compiled from PEER strong motion database. The dataset includes 1,320 and three components accelerograms (two horizontal and one vertical) from 62 earthquakes with magnitudes from 4.7 to 7.6 as shown in Table 3. The fault mechanisms of the earthquakes are referred as: N for normal, SS for strike-slip, R for reverse and RO for reverse-oblique faults. The magnitudes and epicentral distances distributions of the earthquakes records used in the correlation are plotted in Fig. 9. The local site conditions of the records are selected according to preferred NEHRP classification based on Vs30 provided in NGA Peer Data. The functional form for the attenuation relationship is chosen to be the same as that of the CAV5 attenuation relation proposed

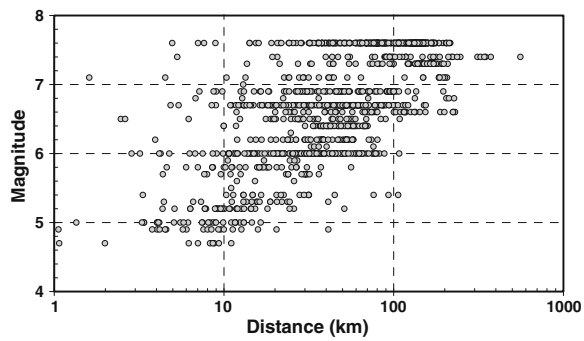

Fig. 9 Distribution of earthquakes records used in attenuation relationship for BCAV-W

Table 4 Correlation equations between BCAV-W and Modified Mercalli Intensity

Window size (s)	Algorithm	c1	c2	c3	c4	f1	f2	h	$\sigma_{\ln(\mathrm{BCAV})}$
4	Max(H1,H2)	13.41	0.50	3.05	−2.26	−0.34	0.26	39.81	0.48
	SRS(H1,H2)	15.60	0.80	0.94	−2.62	−0.34	0.28	51.00	0.49
	SRS(H1,H2,V)	15.41	0.80	0.95	−2.57	−0.27	0.29	48.33	0.48
8	Max(H1,H2)	19.66	0.83	1.58	−3.41	−0.40	0.21	68.38	0.53
	SRS(H1,H2)	27.83	1.00	0.02	−4.82	−0.43	0.20	102.14	0.54
	SRS(H1,H2,V)	27.54	1.08	−0.53	−4.75	−0.37	0.20	99.41	0.53
16	Max(H1,H2)	25.07	1.47	−1.29	−4.41	−0.45	0.15	85.96	0.56
	SRS(H1,H2)	34.13	1.35	−0.93	−5.94	−0.47	0.16	117.98	0.58
	SRS(H1,H2,V)	35.17	1.32	−0.89	−6.11	−0.42	0.16	119.62	0.57
32	Max(H1,H2)	26.87	2.56	−7.07	−4.78	−0.47	0.12	87.78	0.56
	SRS(H1,H2)	35.79	2.45	−6.71	−6.28	−0.48	0.13	117.85	0.59
	SRS(H1,H2,V)	37.99	2.40	−6.53	−6.65	−0.43	0.13	122.99	0.59

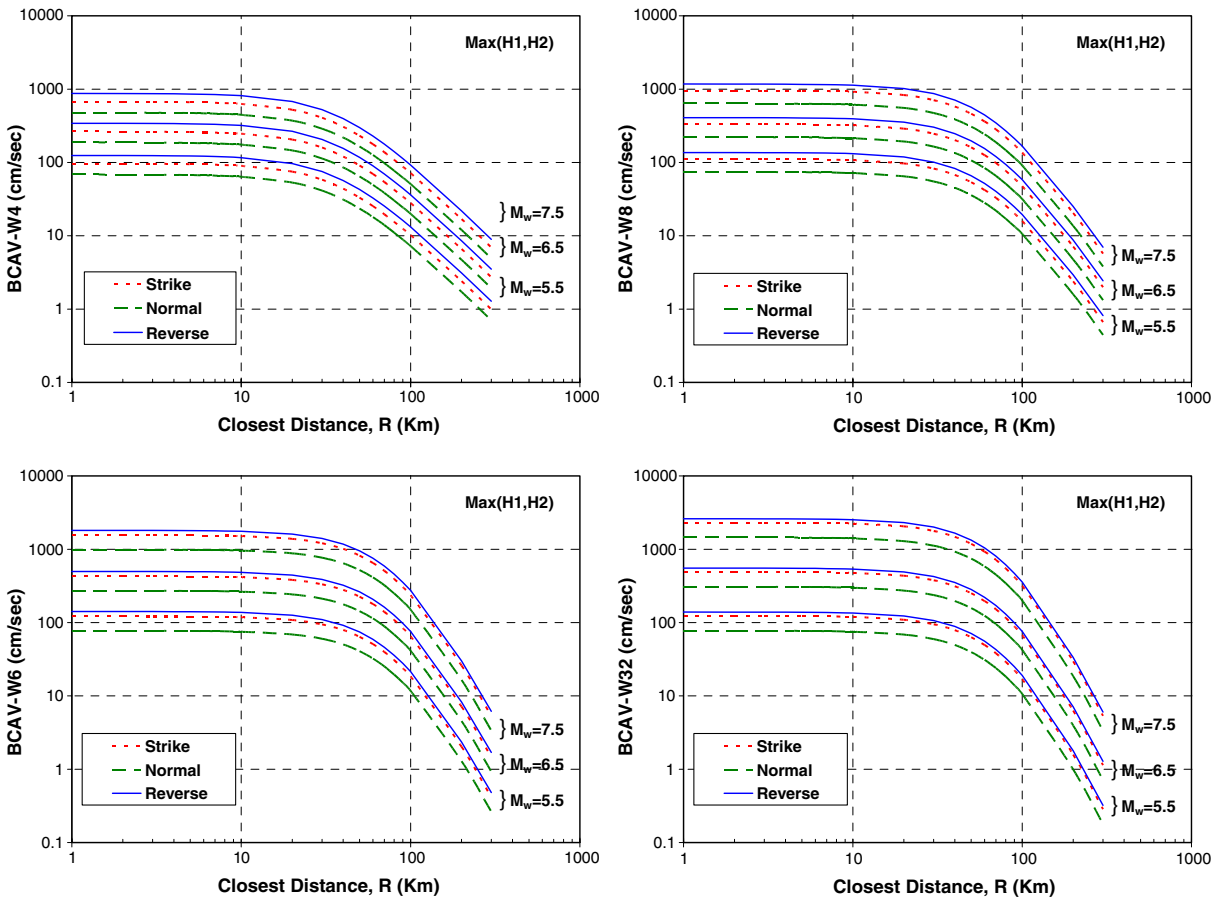

Fig. 10 Median values of BCAV-W versus distance for different magnitudes using Max(H1,H2) algorithm

by Kramer and Mitchell (2006) and Arias intensity attenuation relation developed by Travasarou et al. (2003). The form of the CAV-W attenuation equation is considered as:

$$\ln(\text{BCAV-W}) = c_1 + c_2(M-6) + c_3 \ln(M/6) + c_4 \ln\left(\sqrt{R^2+h^2}\right) + f_1 F_N + f_2 F_R \quad (10)$$

where BCAV-W has units of cm/s, M is the moment magnitude, R is the closest distance to the rupture in km, h is a fictitious hypocentral depth determined by regression, and FN and FR are variables for the fault type (FN = FR = 0 for strike slip faults, FN = 1 and FR = 0 for normal faults, and FN = 0 and FR = 1 for reverse or reverse-oblique faults). The error term associated with Eq. 10 is normally distributed with zero mean and standard deviation σ. The coefficients of the empirical attenuation equation are computed using a nonlinear mixed-effects model (Abrahamson and Youngs 1992) with the aid of the statistical software program S-PLUS (Insightful Corp 2007). A mixed-effects model, with intra and inter-event error terms, was used so that the model coefficients would not be unduly influenced by earthquakes with large numbers of recordings. The resulting coefficients of the regression model for BCAV-W with 8, 16, and 32 s window sizes for different combinations of ground motions components are provided in Table 4. The plots of median values of BCAV-W versus closest distance for the moment magnitudes 5.5, 6.5 and 7.5 and for different fault types; strike-slip, normal and reverse or reverse-oblique faults are shown in Figs. 10, 11 and 12 for

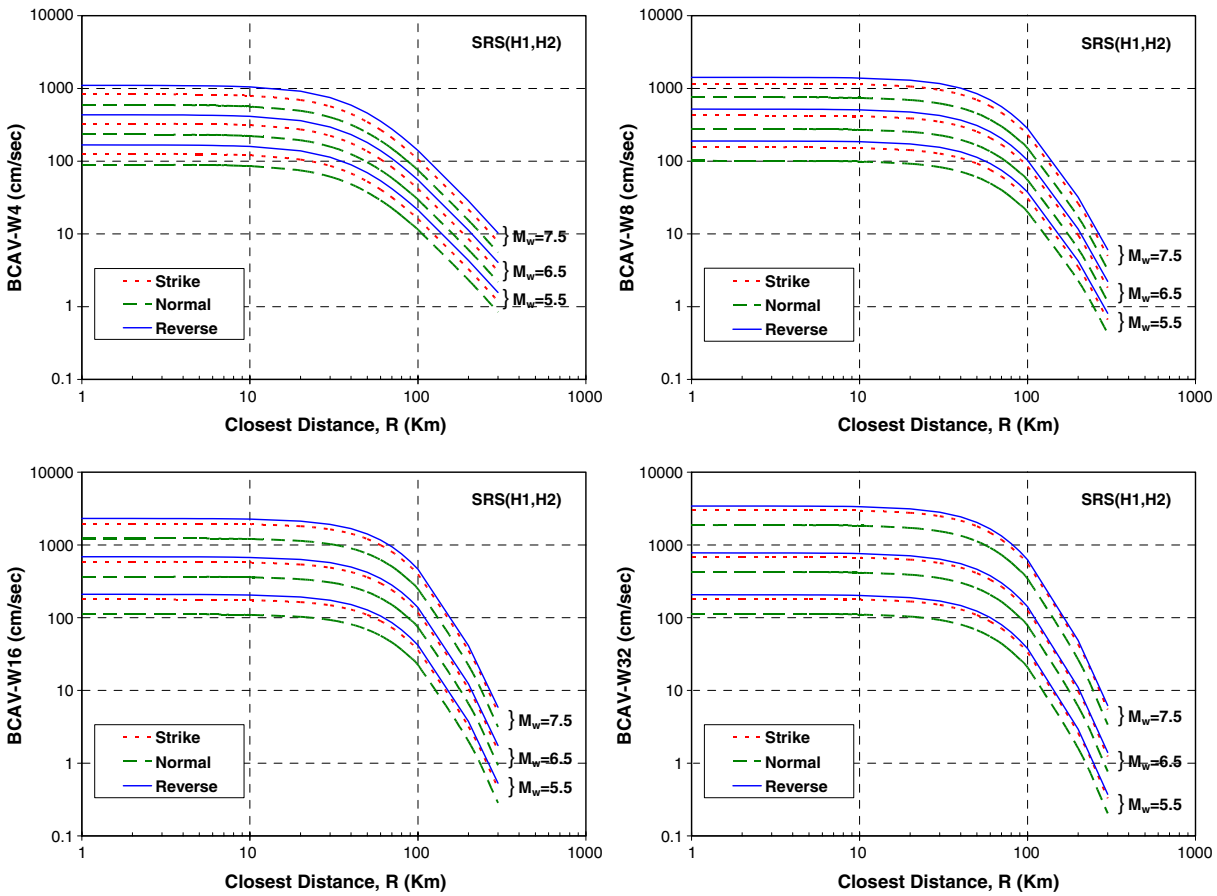

Fig. 11 Median values of BCAV-W versus distance for different magnitudes using SRS(H1,H2) algorithm

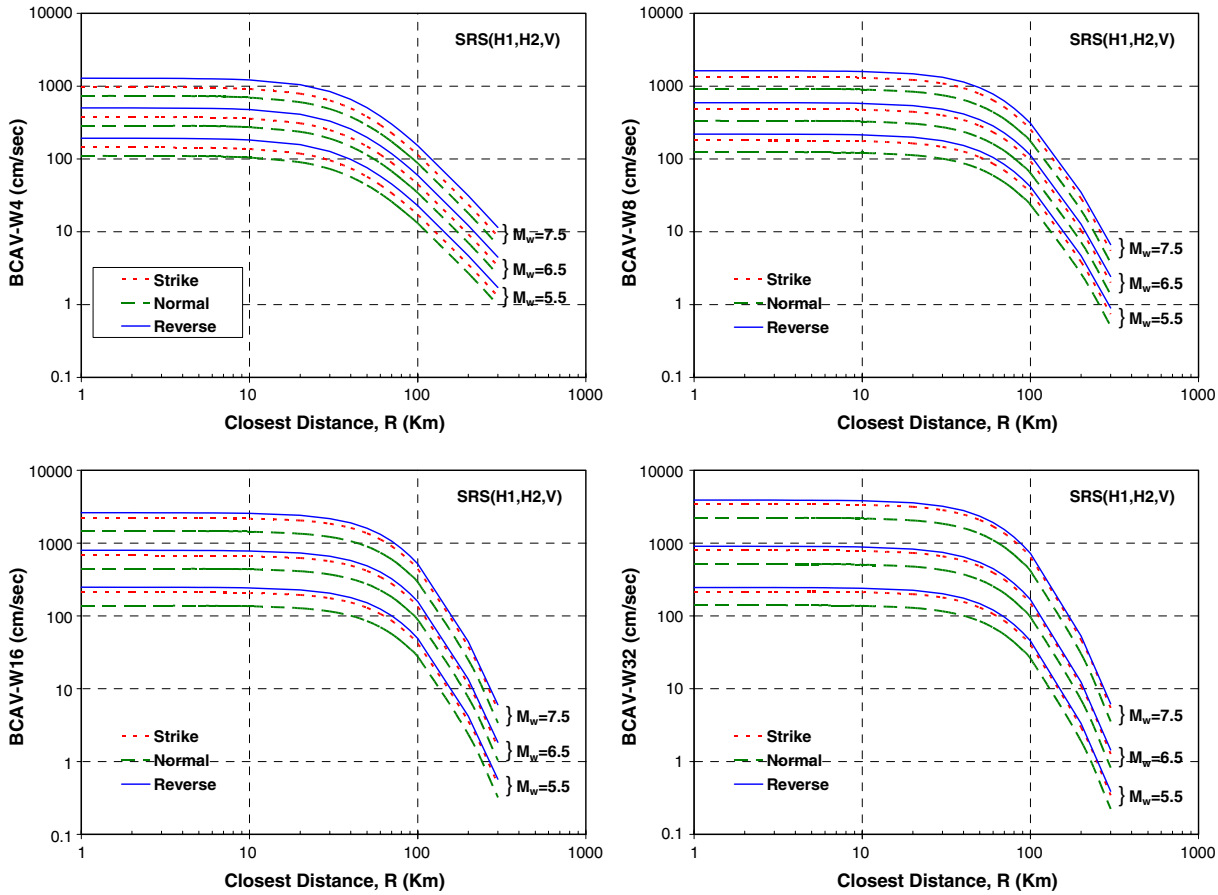

Fig. 12 Median values of BCAV-W versus distance for different magnitudes using SRS(H1,H2,V) algorithm

Max(H1,H2), SRS(H1,H2) and SRS(H1,H2,V) combinations respectively. The plots of attenuation relationships indicate that BCAV-W for all window sizes have almost constant values for the closest distance less than 20 km. The attenuation relationships for reverse faults predict greater values of BCAV-W than strike slip faults and normal faults for all window sizes. The differences

Table 5 The BCAV-W triggering levels proposed for urban early warning system

Window size (s)	Algorithm	Trigger level I (cm/s)	Trigger level II (cm/s)	Trigger level III (cm/s)
4	Max(H1,H2)	80	100	130
	SRS(H1,H2)	100	130	160
	SRS(H1,H2,V)	110	140	170
8	Max(H1,H2)	110	150	200
	SRS(H1,H2)	140	190	250
	SRS(H1,H2,V)	150	210	270
16	Max(H1,H2)	120	180	250
	SRS(H1,H2)	150	230	320
	SRS(H1,H2,V)	160	250	350
32	Max(H1,H2)	130	190	260
	SRS(H1,H2)	160	240	330
	SRS(H1,H2,V)	180	270	360

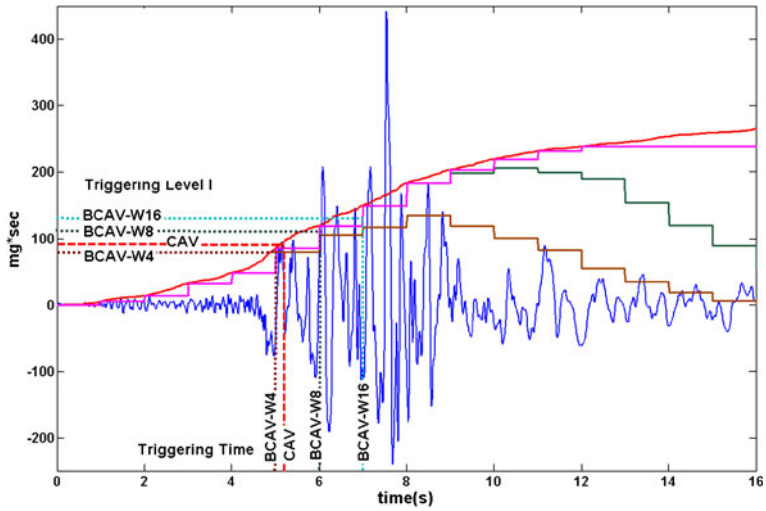

Fig. 13 Triggering levels and triggering time for CAV and BCAV-W

between reverse and strike-slip faults reduce with increasing the window size.

6 Triggering levels, triggering time, and reliability of BCAV-W

In this section, reliability, triggering levels and triggering time for the different algorithms of BCAV-W are studied. The BCAV-W triggering levels for first, second and third alarms can be selected to match the intensities V, VI, and VII of modified Mercalli scale corresponding to rather strong, strong and very strong ground shaking respectively. Considering the mean values and standard deviations of the correlation equations between BCAV-W and modified Mercalli intensity, the three triggering levels for BCAV-W4, BCAV-W8, BCAV-W16 and BCAV-W32 for different algorithms Max(H1,H2), SRS (H1, H2) and SRS(H1,H2,V) are proposed in Table 5. The three triggering levels for CAV are computed using Koliopoulos et al. (1998) predictive relations to be as 90, 150, 250 cm/s. In Fig. 13, triggering time of first triggering level for BCAV-W with window size 4, 8, 16 are computed and compared with CAV for horizontal component (C05085) of Cholame #5 station recorded during the 1966 Parkfield earthquake.

A comprehensive study of triggering time and reliability are performed using 1,320 time histories records of crustal earthquakes compiled from PEER strong motion database with different magnitude, epicentral distances, focal mechanism and soil conditions. The analyses are carried out for two datasets. The first dataset contains 110 records with low peak ground acceleration where no trigger is expected; (PGA) less than 30 mg.

Table 6 Average triggering time for BCAV-W and CAV for records with PGA <30 mg

Algorithm		Trigger level I		Trigger level II		Trigger level III	
		Average trig. time	Number of trig. events	Average trig. time	Number of trig. events	Average trig. time	Number of trig. events
CAV		26.10	80	28.53	61	32.64	32
BCAV-W4, W8, W16	Max(H1,H2)	0	0	0	0	0	0
	SRS(H1,H2)	0	0	0	0	0	0
	SRS(H1,H2,V)	0	0	0	0	0	0
BCAV-W32	Max(H1,H2)	26.6	1	0	0	0	0
	SRS(H1,H2)	21.80	11	25.81	1	0	0
	SRS(H1,H2,V)	22.19	13	27.32	2	0	0

Table 7 Average triggering time for BCAV-W and CAV for records with PGA >50 mg

Algorithm		Trigger level I		Trigger level II		Trigger level III	
		Average trig. time	Number of trig. events	Average trig. time	Number of trig. events	Average trig. time	Number of trig. events
CAV		4.52	1032	7.22	957	11.62	812
BCAV-W4	Max(H1,H2)	4.60	875	4.93	723	4.93	555
	SRS(H1,H2)	6.43	938	6.88	795	7.02	663
	SRS(H1,H2,V)	5.65	940	6.15	784	6.43	642
BCAV-W8	Max(H1,H2)	5.43	947	6.15	767	6.17	593
	SRS(H1,H2)	6.15	1000	7.25	869	7.93	682
	SRS(H1,H2,V)	6.81	1009	8.04	863	8.54	693
BCAV-W16	Max(H1,H2)	5.88	958	7.68	857	8.80	693
	SRS(H1,H2)	6.25	1001	8.13	912	9.87	788
	SRS(H1,H2,V)	6.77	1015	8.82	931	10.53	800
BCAV-W32	Max(H1,H2)	6.22	945	8.08	847	9.88	727
	SRS(H1,H2)	6.53	992	8.41	904	10.47	823
	SRS(H1,H2,V)	7.26	1001	9.26	916	11.23	850

The second dataset compose of 1,068 records with moderate to high peak ground accelerations; PGA greater than 50 mg. The distribution of second dataset records with respect to PGA is as follows: 211 records with PGA less than 75 mg; 170 records with PGA between 75 mg and 100 mg, and 687 records with PGA greater than 100 mg.

All records of the first dataset are analyzed in terms of triggering time using different algorithms and the results are summarized in Table 6. The results demonstrate that CAV may give false alarms for records with low (non-damaging) ground accelerations due to accumulation of absolute velocity with the time for long duration records. Eventhough BCAV-W algorithms with window sizes of 4, 8, and 16 do not result in any alarms, BCAV-W32 results in few alarms for the first triggering level and very few alarms for the second triggering level.

The analyses results for the second dataset are presented in Table 7. The small window size BCAV-W4 given the fastest trigger but with less number of triggering events. In general, BCAV-W with different windows size give alarm for all the records with PGA greater than 70 mg. Selecting small window size (4 s) are appropriate for fast triggering, however increasing the window size enhance the reliability for the algorithm, but there is no significant benefit to choose a window size more than 16 s. For all window sizes, the maximum of horizontal components, Max (H1, H2) algorithm gives the fastest triggering time, on the other hand, square root of sum squares of three components, SRS (H1, H2, V) is the most reliable algorithm.

7 Conclusion

In this study, window-based BCAV-W definition are proposed for online urban earthquake early warning systems in order to allow a continuous operation in a specific moving window size and to include the vertical component of the motion. The major operational merit for the new BCAV-W definition can be summarized as: (1) elimination of the accumulated BCAV values due to different reasons, for examples: high noises, small earthquakes and far field events, (2) adjustment of the minimum acceleration level which is originally proposed for nuclear power plants, (3) identification of the short time earthquake motions with very large peak ground accelerations (near-field impulsive) from long time earthquake motions with a lower acceleration level (far field). The size of the moving window for BCAV-W can be selected taken into account the spatial variation of the seismic stations and the distance between the potential source zone and the urban area. For urban early warning systems, diferent combination using the three components of the free-field ground motion (i.e., two horizontal

and one vertical) can be used. Classically, the maximum of the horizontal components of the motions is considered for early warning system of nuclear power plants where in most cases the seismic stations are located in the vicinity of the plant. In an urban early warning system where the seismic stations located as close as possible to the potential fault source zone, it is useful to consider the effect of both horizontal and vertical components of the ground motions. Therefore, different triggering algorithms can be considered using a different combination of the three components of the free-field ground motion: (1) Maximum of Horizontal Components, Max (H1, H2); 2) Square Root of Sum Squares of Horizontal Components, SRS (H1, H2); 3) Square Root of Sum Squares of Three Components, SRS (H1, H2, V). The attenuation relationships of BCAV-W indicate that all window sizes have almost constant values for the closest distance less than 20 km and the attenuation relationships for reverse faults predict greater values of BCAV-W for all window sizes than strike slip faults and normal faults.

Selecting small window size (4 s) are appropriate for fast triggering, however, increasing the window size enhance the reliability for the algorithm, but there is no significant benefit to choose a window size more than 16 s. For all window sizes, the maximum of horizontal components, Max (H1, H2) algorithm gives the fastest triggering time, but the square root of sum squares of three components, SRS (H1, H2, V) is the most reliable algorithm.

Acknowledgements The author would like to thank Prof. Dr. Mustafa Erdik for suggesting the research topic.

References

Abrahamson NA, Youngs RR (1992) A stable algorithm for regression analyses using the random effects model. Bull Seismol Soc Am 82(1):505–510

Alcik H, Fahjan YM, Erdik M (2006) Analysis of Triggering Algorithms for Direct (Engineering) Early Warning Systems. In: First European Conference on Earthquake Engineering and Seismology, Geneva, Switzerland, 3–8 September 2006

Allen RM, Kanamori H (2003) The potential for earthquake early warning in Southern California. Science 300:786–789

Ashiya K (2004) Earthquake alarm systems in Japan railways. Journal of Japan Association for Earthquake Engineering 4(3) (Special Issue):112–117

Cabanas L, Benito B, Herraiz M (1997) An approach to the measurement of the potential structural damage of earthquake ground motions. Earthq Eng Struct Dyn 26:79–92

Cansi Y (1995) An automatic seismic event processing for detecting and location the P.M.C.C. method. Geophys Res Lett 22:1021–1024

EPRI (1988) A Criterion for determining exceedance of the operating basis earthquake. In: Electric Power Research Institute, Palo Alto, CA, prepared by Jack R. Benjamin and Associates Inc, Report No: NP-5930

EPRI (1991) Standardization of the cumulative absolute velocity. In: Electric Power Research Institute, Palo Alto, CA, prepared by Yankee Atomic Electric Company Report No: TR-100082

EPRI (2006) Use of cumulative absolute velocity (CAV) in determining effects of small magnitude earthquakes on seismic hazard analyses. In: Electric Power Research Institute, Electric Power Research Institute, Palo Alto, CA, prepared by ARES Corporation Inc and Norm A Abrahamson Inc, Report No: RS-1014099

Erdik M, Fahjan YM, Ozel O, Alcik H, Mert A, Gul M (2003) Istanbul earthquake rapid response and the early warning system. Bulletin of Earthquake Engineering 1(1):157–163

Espinosa-Aranda J, Jimenez A, Ibarrola G, Alcantar F, Aguilar A, Inostroza M, Maldonado S (1995) Mexico City seismic alert system. Seismol Res Lett 66:42–53

Espinoza-Aranda J, Rodriquez-Cayeros FH (2003) The seismic alert system of Mexico City. In: Lee WHK, Kanamori H, Jennings PC and Kisslinger C (ed) International handbook of earthquake and engineering seismology, Academic, pp 1253–1260

European Strong-Motion Database (2000) Constructed by Imperial College of Science, Technology and Medicine, London, UK; ENEA (SOGIN and SSN), Rome, Italy; IPSN, France under European Commission, Research Directorate—General, Environment and Climate Programme, contract ENV4-CT97-0397

Harben PE (1991) Earthquake alert system feasibility study. Lawrence Livermore National Laboratory, Livermore, CA, Report No:UCRL-LR-109625

Heaton TH (1985) A model for seismic computerized alert network. Science 228:987–990

Horiuchi S, Matsuzawa T, Hasegawa A (1992) A real-time processing system of seismic wave using personal computers. J Phys Earth 40:395–406

Horiuchi S, Negishi H, Abe K, Kamimura A, Fujinawa Y (2005) An automatic processing system for broadcasting earthquake alarms. Bull Seismol Soc Am 95(2):708–718

Insightful Corporation (2007) S-PLUS version 8. Seattle, WA

Kanamori H (1993) Locating earthquakes with amplitude: application to real-time seismology. Bull Seismol Soc Am 83:264–268

Kanamori H, Hauksson E, Heaton T (1997) Real-time seismology and earthquake hazard mitigation. Nature 390:461–464

Koliopoulos PK, Margaris BN, Klimis NS (1998) Duration and energy characteristics of Greek strong motion records. J Earthqu Eng 2:391–417

Kostov MK (2005) Site specific estimation of cumulative absolute velocity. In: 18th International Conference on Structural Mechanics in Reactor Technology (SMiRT 18), Beijing, China, August 7–12, 2005

Kramer SL (1996) Geotechnical earthquake engineering. Prentice Hall, New Jersey

Kramer SL, Mitchell RA (2006) Ground motion intensity measures for liquefaction hazard evaluation. Earthq Spectra 22(2):413–438

Lee J-R, Lee S-H (2001) An experimental study on seismic damage indicator considering CAV concept. Transactions, SMiRT 16, Washington DC, August 2001, Paper # 1776

Nakamura Y (1988) On the urgent earthquake detection and alarm system (UrEDAS). In: Proc of the 9th World Conference on Earthquake Engineering VII, Tokyo, Japan, 2–9 August 1988, 673–678

Ozmen B (2000) Isoseismal map, human casualty and building damage statistics of The Izmit earthquake of August 17, 1999. In: Third Japan–Turkey Workshop on Earthquake Engineering, February 21–25, 2000, Istanbul, Turkey

Shabestari KT, Yamazaki F (2001) A proposal of instrumental seismic intensity scale compatible with MMI evaluated from three-component acceleration records. Earthq Spectra 17(4):711–723

Sokolov VY (2002) Seismic intensity and Fourier acceleration spectra: revised relationship. Earthq Spectra 18(1):161–187

Sokolov VY, Chernov YK (2002) On the correlation of the seismic intensity with FAS. Earthq Spectra 14(4):679–694, 1998.

Teng TL, Wu YM, Shin TC, Tsai YB, and Lee WHK (1997) One minute after: strong-motion map, effective epicenter, and effective magnitude. Bull Seismol Soc Am 87:1209–1219

Travasarou T, Bray JD, Abrahamson NA (2003) Empirical attenuation relationship for Arias Intensity. Earthq Eng Struct Dyn 32:1133–1155 (doi:10.1002/eqe.270)

Wenzel F, Oncescu MC, Baur M, Fiedrich F (1999) An early warning system for Bucharest. Seismol Res Lett 70(2):161–169

Wu YM, Kanamori H (2005) Experiment on an onsite early warning method for the Taiwan early warning system. Bull Seismol Soc Am 95:347–353

Wu YM, Shin TC, Tsai YB (1998) Quick and reliable determination of magnitude for seismic early warning. Bull Seismol Soc Am 88:1254–1259

Yokota T, Zhou S, Mizoue M, Nakamura I (1981) An Automatic measurement of arrival time of seismic waves and its application to an online processing system. Bull Earthq Res Ins 55:449–484